Physical Modelling in Geotechnics

Numerical simulation of centrifuge model tests on reduction of coefficient of horizontal subgrade reaction of piles in liquefied volcanic ash ground

T. Egawa & H. Hayashi
Civil Engineering Research Institute for Cold Region, Sapporo, Japan

K. Isobe
Hokkaido University, Sapporo, Japan

ABSTRACT: To clarify how differences in the state of deposition of volcanic ash soil affect the tendency for the coefficient of horizontal subgrade reaction of the piles to be reduced, a dynamic effective stress analysis (LIQCA 3D) that reproduced the results of a centrifuge model test on piles in liquefaction-prone volcanic ash soil layers of different thicknesses and structures was performed. The experimental results were accurately reproduced, including the tendency for the amplitudes of the piles and the ground to attenuate with liquefaction, by considering the pile volume, the damping constant based on the natural frequency of the pile and ground, and the liquefaction parameters corresponding to the effective confining pressure of the ground, and also by applying the effective stress model to the dense sand layer, too. In the experiment case in which a great reduction in the coefficient of horizontal subgrade reaction of the pile at liquefaction was observed, it was found that a great shear strain was generated in the ground and that there was a drastic decrease in the shear modulus caused by a drastic increase in the excess pore water pressure.

Keywords: volcanic ash soil, liquefaction, coefficient of horizontal subgrade reaction of pile, centrifuge model test, numerical simulation.

1 INTRODUCTION

Hokkaido is the northernmost island of Japan, and more than 40% of its total area is covered with unconsolidated volcanic products of diverse sources and depositional conditions. The 2018 Hokkaido Eastern Iburi Earthquake caused enormous damage to structures due to the liquefaction of volcanic ash ground. To mitigate the potential damage caused by a future major earthquake, it is important to evaluate in advance the effect of the differences in the depositional status of the liquefiable volcanic ash soil layer on the structural foundation. To develop the evaluation method, Egawa et al. (2018) conducted a series of centrifugal model tests of volcanic ash soil layers with variations in the deposition of ash soil and the occurrence of liquefaction. The same seismic motion was input from the base in all five cases shown in Figure 1 and Table 1. As a result, it was confirmed that the coefficient of horizontal subgrade reaction of piles was more significantly reduced in Case 2 and Case 4 than in the other cases. The following causes were inferred in consideration of the test results. In Case 2, the natural frequency of the ground was close to the input frequency, and the shear strain that occurred relatively continuously in all layers promoted liquefaction and a decrease in the rigidity of the ground. In Case 4, the excess pore water pressure that rose sharply in the middle layer was propagated to the upper layer and greatly reduced the initial rigidity of the upper layer.

In this study, dynamic effective stress analysis program (LIQCA) was used to simulate the centrifuge model tests and to clarify the factors inferred from the tests.

2 CENTRIFUGE MODEL TESTS

Dynamic centrifuge model tests were conducted in $50g$ of centrifugal force field. Figure 1 shows the outline of the model tests. Before the shaking tests, a static horizontal loading tests were conducted to confirm the coefficient of static horizontal subgrade reaction of piles. For the volcanic ash soil, the Shikotsu pumice flow deposit Spfl, which was liquefied on a large scale during the 2018 Hokkaido Eastern Iburi Earthquake, was used. For more details on materials and the model preparation method, see Egawa et al. (2018).

3 DYNAMIC EFFECTIVE STRESS ANALYSIS

A dynamic effective stress analysis program, LIQCA, developed by Oka et al. (1991) was used to simulate the tests results. Figure 2 shows the analytical model (using Case 2 as an example).

3.1 Analytical model basic settings

The analytical model was set as a half cross-section in consideration of the symmetry of the test model. A vertical roller was used for the side surface of the model, and the bottom surface of the model was fixed. To fix the piles, they were completely constrained at the bottom to prevent displacement and rotation, and the boundary between the weight and the piles was constrained to prevent rotation. No joint elements were introduced at the boundary between the piles and the ground since the target is liquefied ground, where the rigidity of the ground around the piles decreases largely and the influence of discontinuous behavior of the boundary becomes relatively small. The acceleration waveform measured on each case base in the dynamic shaking test was used as an input acceleration waveform.

3.2 Pile modeling

Pile modeling and parameter settings were examined based on the simulation analysis of the shaking test of piles only, in which a ground model was not created in the test model. The piles were used as elastic beam elements as they showed elastic behavior in the test, and the volume of the piles was considered using equal displacement constraint (MPC constraint). For the Rayleigh damping of piles, the damping constant $h = 2\%$ is assumed for the natural frequency f of piles obtained from the shaking test of piles only, and a rigidity proportional damping constant $\alpha_1 = 0.0126$ was set. As a result, the behavior of piles only was reproduced relatively well.

3.3 Ground modeling

As for modeling of the ground, the results of the shaking test showed that excessive pore water pressure was generated even in dense sandy soil as a non-liquefaction layer, so the liquefaction layer (volcanic ash soil D_r = 85%) and the non-liquefaction layer (Toyoura sand D_r = 95%) were set as cyclic elasto-plasticity models (effective stress model). In addition, settings were made in consideration of the constraint pressure dependency of the ground materials.

In consideration of the constraint pressure dependency, the ground models and various parameters were set based on the results of the cyclic undrained triaxial test on soils (JGS0541-2020) and the cyclic triaxial test to determine the deformation properties of soils (JGS0542-2020) and were conducted by dividing the entire thickness of the ground into the three layers of upper, middle, and lower, and at an effective confining pressure close to the middle depth of each layer. In this study, the effective confining pressure σ'_0 for each of the upper, middle, and lower layers was set as 15kPa, 50kPa, 75kPa in the liquefaction layer and 30kPa, 50kPa, and 100kPa in the non-liquefaction layer.

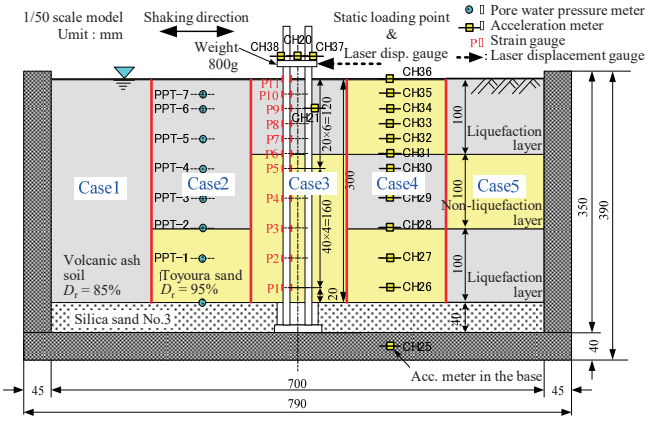

Fig. 1. Outline of the test model.
(Five cases are shown in section for the sake of comparison.)

Table 1. Test cases.

Case	Model ground	Relative density D_r (%)	Liquefaction strength ratio R_{L20}	Thickness (m)	Input seismic motion
1	Volcanic ash soil	85	0.242	15.0	20 sine waves
2	Volcanic ash soil	85	0.242	10.0	
	Toyoura sand	95	-	5.0	Frequency
3	Volcanic ash soil	85	0.242	5.0	1.5Hz
	Toyoura sand	95	-	10.0	
4	Toyoura sand	95	-	5.0	Max. Acc.
	Volcanic ash soil	85	0.242	5.0	200cm/s^2
	Toyoura sand	95	-	5.0	
5	Volcanic ash soil	85	0.242	5.0	
	Toyoura sand	95	-	5.0	
	Volcanic ash soil	85	0.242	5.0	

* in Prototype scale

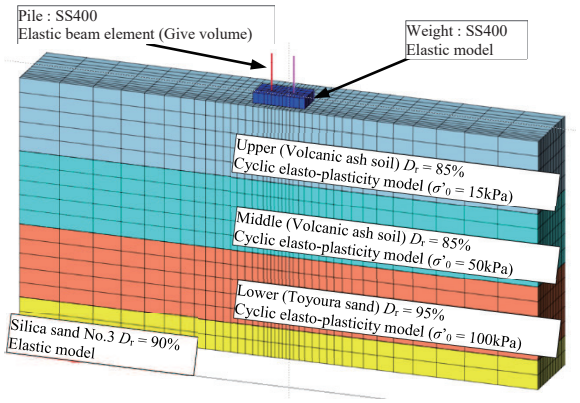

Fig. 2. LIQCA analytical models (Example of Case 2).

Table 2. Typical liquefaction parameters (Example of Case 2).
(Determined from element simulations.)

Parameter	Upper layer Volcanic ash soil D_r = 85%	Middle layer Volcanic ash soil D_r = 85%	Lower layer Toyoura sand D_r = 95%
Initial void ratio e_0	1.163	1.163	0.658
Coefficient of permeability k (m/s)	5.21E-06	5.21E-06	1.41E-04
Compression index λ	0.0200	0.0200	0.0028
Swelling index κ	0.0051	0.0051	0.0018
Stress ratio at Max. Compression M_m^*	1.023	1.023	0.803
Dilatancy coefficient D^*	2.5	3.0	1.6
Dilatancy coefficient n	2.0	3.5	1.0

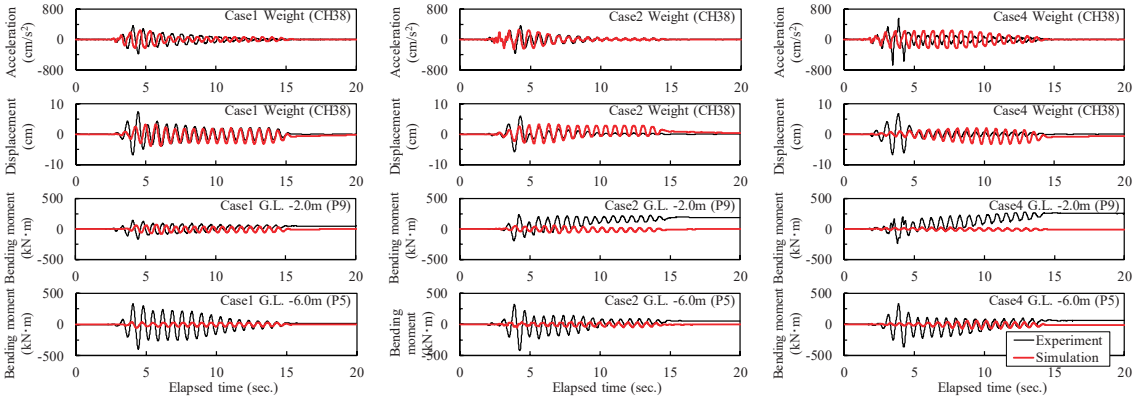

Fig. 3. Time history of acceleration and displacement of pile head weight and bending moment of piles in the ground (Cases 1, 2 and 4).

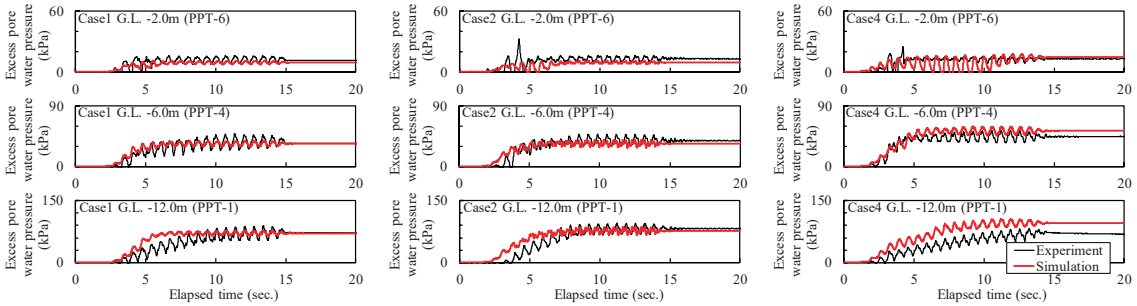

Fig. 4. Time history of excess pore water pressure in the ground (Cases 1, 2, and 4).

Table 2 shows the liquefaction element simulation results when parameters were set with an emphasis on matching the stress path of the JGS0541-2020 results. The compression index λ, swelling index κ, and dilatancy coefficients D^* and n determined based on the element simulations were larger in volcanic ash soil than Toyoura sand. A gradual decrease in effective stress was also reproduced by offsetting with a large initial void ratio e_0. For the Rayleigh damping of the ground, the shear wave velocity V_S of each layer was obtained from the natural frequency f of the ground found with the shaking test in each case and the shear modulus of rigidity G_0 of JGS0542-2020 carried out at each confining pressure, and α_1 was set for each layer in each case based on the relational expression ($h = 7.5/V_S$) with the damping constant h. The stress ratio at maximum compression M_m^* which is one of the parameters of the ground, was set based on the phase transformation angle of the triaxial compression test (CUber) on soil (JGS0523-2020) of each ground material.

4 ANALYSIS AND TESTS RESULTS

Figures 3 and 4 show the time history of the main analysis results of Cases 1, 2 and 4 as typical examples in comparison with the test results.

In Figure 3, the response acceleration of weights at pile heads show a relatively good match with the test results, and the damping tendency is also reproduced. Displacement of the weights at the pile heads was confirmed to differ from the test results in the early stage of shaking, but the amplitude values, phase, and damping tendency after the early stage of shaking showed good

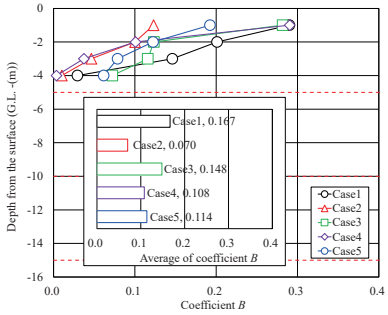

Fig. 5. Reduction coefficient B of the horizontal subgrade reaction coefficient of piles due to liquefaction.

matching. The bending moment of the piles in the ground is also underestimated as a whole and cannot be said to be accurate. It is considered that in the test, the pile showed rotation behavior due to the shaking, and it is necessary to also consider reproduction of the rotational behavior in the future.

In Figure 4, excess pore water pressure in the ground accurately reproduces the test results and the behavior of the non-liquefaction layer. The improvement of analysis accuracy was recognized by setting the liquefaction parameters and damping constants according to the effective confining pressure. In particular, it was suggested that it is appropriate to use the effective stress model even for dense sandy soil (non-liquefaction layer).

Figure 5 shows the reduction coefficient B of the horizontal subgrade reaction coefficient of piles due to liquefaction obtained using the analysis results of all five cases. Using the method of obtaining the reduction coefficient B from the test and analysis results (Egawa et al., 2018), the horizontal subgrade reaction coefficient of piles is calculated from the bending moment of piles, so the value of coefficient B obtained from the analysis

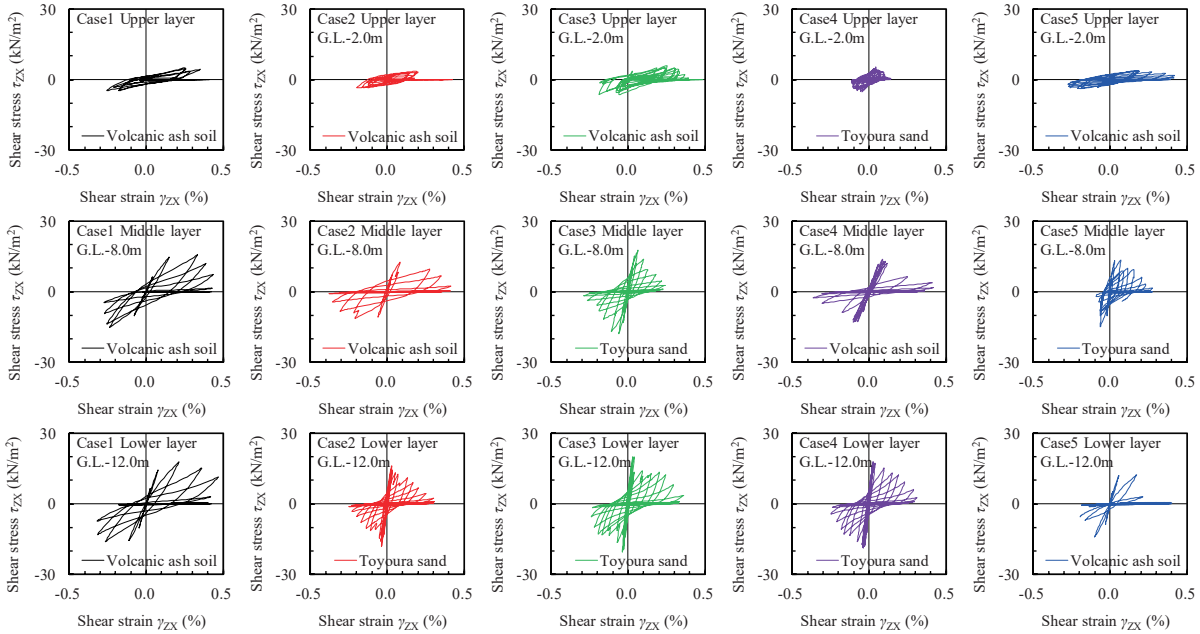

Fig. 6. Shear stress-shear strain relationship of the ground in the upper (G.L.- 2.0m), middle (G.L.- 8.0m) and lower (G.L.- 12.0m) layers.

results was overall smaller than the test results. However, in Cases 2 and 4, the same tendency as in the test results was confirmed in which the horizontal subgrade reaction coefficient of piles was lower than in other cases.

Since the tendency of the test was reproduced relatively well by the analysis, we considered the differences between Case 2 or 4 and other cases from the shear stress-shear strain relationship in the ground obtained by the analysis.

Figure 6 shows the shear stress-shear strain relationship in the ground in response to 20 seismic waves at the middle depth of each of the upper, middle, and lower layers in all five cases obtained by analysis.

In Figure 6, it can be confirmed that in the lower layer, the rigidity at the initial stage of shaking in each case gradually decreases while showing relative elasticity.

Meanwhile, in the middle layer, shear strain is predominant in Case 2 from the early stage of shaking, and the rigidity is lower than in other cases. In Case 4, the rigidity is maintained at the initial stage of shaking, but then drops sharply. It can also be seen that the shear strain generated in both cases was larger in the middle than the lower layer. This is considered to be due to the fact that the initial rigidity of the lower layer is larger than that of the middle layer in both cases, the influence of the difference in rigidity, and the rapid increase in excess pore water pressure in Case 4.

In the upper layer, the gradient of the hysteresis curve is small from the initial stage of shaking in each case, but in Cases 1 and 3, it is confirmed that the rigidity was maintained or restored during shaking. In Cases 2 and 4, the size of the hysteresis curve was small, but there were many hysteresis curves that are almost horizontal, showing that the rigidity was significantly lower in these than other cases.

These facts are considered to be in good agreement with the inferences from the test results.

5 CONCLUSIONS

- The test results, such as the tendency of the amplitudes of piles and ground to decay with liquefaction, were reproduced with relatively high accuracy taking the volume of the pile into consideration, setting the damping constant based on the natural frequency of piles and the liquefaction parameters and damping constants according to the effective confining pressure of the ground and the natural frequency, especially when using the effective stress model even in a dense sandy soil layer as a non-liquefaction layer.
- The results of analysis confirmed that the horizontal subgrade reaction coefficient of the piles in Case 2 and Case 4 tends to be smaller than in other cases, corresponding with the tendency demonstrated by the test results. Analysis verified a tendency in good agreement with the inferences from the test results showing that in Case 2, the shear strain that occurred relatively continuously in all layers promoted liquefaction and reduced the rigidity of the ground, and in Case 4, excess pore water pressure that rose sharply in the middle layer was propagated, with a significant drop in the initial rigidity of the upper layer.

REFERENCES

Egawa, T., Yamanashi, T. & Isobe, K. 2018. Investigation on the aseismic performance of pile foundations in volcanic ash ground. *9th International Conference on Physical Modelling in Geotechnics*, 879-884.

Oka, F., Yashima, A., Shibata, T. & Kato, M. 1991. A finite element analysis of liquefaction of seabed due to wave action. *Geo-Coast'91*, 621-626.